Physics Letters B 740 (2015) 158–167

Contents lists available at ScienceDirect

Physics Letters B

www.elsevier.com/locate/physletb

Search for *CP* violation in $D^0 \to \pi^-\pi^+\pi^0$ decays with the energy test

LHCb Collaboration

ARTICLE INFO

Article history:
Received 17 October 2014
Received in revised form 17 November 2014
Accepted 20 November 2014
Available online 25 November 2014
Editor: W.-D. Schlatter

ABSTRACT

A search for time-integrated *CP* violation in the Cabibbo-suppressed decay $D^0 \to \pi^-\pi^+\pi^0$ is performed using for the first time an unbinned model-independent technique known as the energy test. Using proton–proton collision data, corresponding to an integrated luminosity of 2.0 fb^{-1} collected by the LHCb detector at a centre-of-mass energy of $\sqrt{s} = 8$ TeV, the world's best sensitivity to *CP* violation in this decay is obtained. The data are found to be consistent with the hypothesis of *CP* symmetry with a *p*-value of $(2.6 \pm 0.5)\%$.

1. Introduction

The decay $D^0 \to \pi^-\pi^+\pi^0$ (charge conjugate decays are implied unless stated otherwise) proceeds via a singly Cabibbo-suppressed $c \to du\bar{d}$ transition with a possible admixture from a penguin amplitude. The interference of these amplitudes may give rise to a violation of the charge-parity symmetry (*CP* violation), which may be observed as an asymmetry in the total rates, or in the distribution of events over the Dalitz plot. Contributions from particles that are not described in the Standard Model (SM) and participate in the loops of the penguin amplitude can enhance the $O(10^{-3})$ *CP* violation effects expected within the SM [1]. Therefore *CP* violation in $D^0 \to \pi^-\pi^+\pi^0$ decays provides sensitivity to such non-SM physics.

In addition to this direct *CP* violation, time-integrated *CP* asymmetry in $D^0 \to \pi^-\pi^+\pi^0$ decays can also receive an indirect contribution arising from either the D^0–$\overline{D}^0$ mixing or interference in decays following mixing. While direct *CP* asymmetry depends on the decay mode, indirect *CP* violation is expected to be the same for all *CP* eigenstates. Recent time-dependent measurements of $D^0 \to \pi^-\pi^+$, K^-K^+ decays constrain the indirect *CP* asymmetry to the $O(10^{-3})$ level [2].

The decay $D^0 \to \pi^-\pi^+\pi^0$ is dominated by the $\rho(770)$ resonances, with the ρ meson decaying into a pair of pions, which lead to the final states $\rho^0\pi^0$, $\rho^+\pi^-$, and $\rho^-\pi^+$. Higher-mass ρ and f_0 resonances, as well as $f_2(1270)$ and $\sigma(400)$ particles only contribute with fractions at the percent level or less [3].

Singly Cabibbo-suppressed charm decays have recently received a significant attention in the literature (see e.g. Ref. [1]). A particular interest in the decay $D^0 \to \pi^-\pi^+\pi^0$ was pointed out in Ref. [4], where the authors derived isospin relations between the different $D \to \rho\pi$ amplitudes and discussed the possibility of identifying contributions from non-SM physics using *CP* violation measurements.

Previously, the most sensitive search for *CP* violation in this decay was performed by the BaBar Collaboration [5]. Their result excluded *CP*-violating effects larger than a few percent. The results presented here are based on a signal sample that is about eight times larger and have higher precision. This is the first *CP* violation analysis performed at the LHCb experiment with decays involving π^0 mesons.

As $\pi^-\pi^+\pi^0$ is a self-conjugate final state and accessible to both D^0 and $\overline{D}^0$ decays, flavour tagging of the D mesons is performed through the measurement of the soft pion (π_s) charge in the $D^{*+} \to D^0\pi_s^+$ decay.

The method exploited in this Letter, called the energy test [6,7], verifies the compatibility of the observed data with *CP* symmetry. It is sensitive to local *CP* violation in the Dalitz plot and not to global asymmetries. The unbinned technique applied here is used for the first time. A visualisation method is also used that allows identification of regions of the Dalitz plot in which *CP* violation is observed. As this model-independent method cannot identify which amplitudes contribute to the observed asymmetry, a model-dependent analysis would be required in the case of a signal for a non-zero *CP* asymmetry.

2. Detector and reconstruction

The LHCb detector [8] is a single-arm forward spectrometer covering the pseudorapidity range $2 < \eta < 5$, designed for the study of particles containing b or c quarks. The detector includes a high-precision tracking system consisting of a silicon-strip vertex detector surrounding the pp interaction region, a large-area silicon-strip detector located upstream of a dipole magnet with a bending power of about 4 Tm, and three stations of silicon-strip detectors and straw drift tubes placed downstream of the magnet. The combined tracking system provides a measurement of momentum, p, with a relative uncertainty that varies from 0.4% at low

http://dx.doi.org/10.1016/j.physletb.2014.11.043

momentum to 0.6% at 100 GeV/c. The minimum distance of a track to a primary vertex, the impact parameter (IP), is measured with a resolution of $(15 + 29/p_{\mathrm{T}})$ μm, where p_{T} is the component of p transverse to the beam, in GeV/c. Charged hadrons are identified using two ring-imaging Cherenkov detectors. Photon, electron and hadron candidates are identified by a calorimeter system consisting of scintillating-pad and preshower detectors, an electromagnetic calorimeter and a hadronic calorimeter. Muons are identified by a system composed of alternating layers of iron and multiwire proportional chambers.

The trigger consists of a hardware stage, based on high-p_{T} signatures from the calorimeter and muon systems, followed by a two-level software stage, which applies partial event reconstruction. The software trigger at its first level requires at least one good quality track associated with a particle having high p_{T} and high χ^2_{IP}, defined as the difference in χ^2 of the primary pp interaction vertex (PV) reconstructed with and without this particle.

A dedicated second-level trigger partially reconstructs $D^0 \to \pi^-\pi^+\pi^0$ candidates coming from $D^{*+} \to D^0\pi_s^+$ decays using only information from the charged particles. These requirements ensure the suppression of combinatorial background without distorting the acceptance in the decay phase space. The $\pi^-\pi^+$ pair is combined with a pion to form a D^{*+} candidate, which is accepted if it has p_{T} greater than 2.5 GeV/c and a difference of invariant masses $m(\pi^-\pi^+\pi_s^+) - m(\pi^-\pi^+) < 285$ MeV/c^2. All the charged-particle tracks used must have good quality, $p_{\mathrm{T}} > 0.3$ GeV/c and $p > 3.0$ GeV/c, while the charged pions from the D^0 decays must also have high χ^2_{IP}. The $\pi^-\pi^+$ combination is required to form a good quality secondary vertex significantly displaced from the PV, while the soft pion must originate from the PV.

The inclusive D^{*+} trigger was introduced at the start of 2012. The data collected by the LHCb experiment in 2012 corresponds to an integrated luminosity of 2 fb^{-1} of pp collisions collected at a centre-of-mass energy of 8 TeV. The magnetic field polarity is reversed regularly during the data taking with approximately half the data collected at each polarity to reduce the overall effect of any charge-dependent detection and reconstruction efficiency.

In this analysis, the two π^0 categories reconstructed in LHCb are exploited [9]. These are pions for which both final state photons are reconstructed separately (resolved pions), as well as pions that have higher momentum (typically $p_{\mathrm{T}} > 2$ GeV/c) and thus a smaller opening angle of the two photons (merged pions). These π^0 mesons are detected in the calorimeter as one merged cluster which is further split into two subclusters based on the expected shape of the photon shower. The merged pions make up about 30% of the reconstructed π^0 mesons. Among the resolved π^0 mesons there are also candidates made of photons which, after interacting with detector material, have converted into an e^+e^- pair. The two π^0 samples provide coverage of complementary regions of the $D^0 \to \pi^-\pi^+\pi^0$ Dalitz plot and thus the use of both contributes significantly to the sensitivity of the analysis.

3. Event selection

The offline selection is split into a pre-selection, which follows the trigger selection, and a selection based on a boosted decision tree (BDT) [10,11]. All the D^{*+} candidates are required to pass both levels of the software trigger. In addition, the pre-selection requires more stringent kinematic criteria than those applied in the trigger; in particular $p_{\mathrm{T}} > 0.5$ GeV/c is required for all the D^0 decay products to reduce the combinatorial background. For resolved π^0 mesons, the di-photon invariant mass has to be within 15 MeV/c^2 of the known π^0 mass, this corresponds to about three times the $m(\gamma\gamma)$ resolution. The invariant mass of merged photons, due to its lower resolution, is required to be within the range

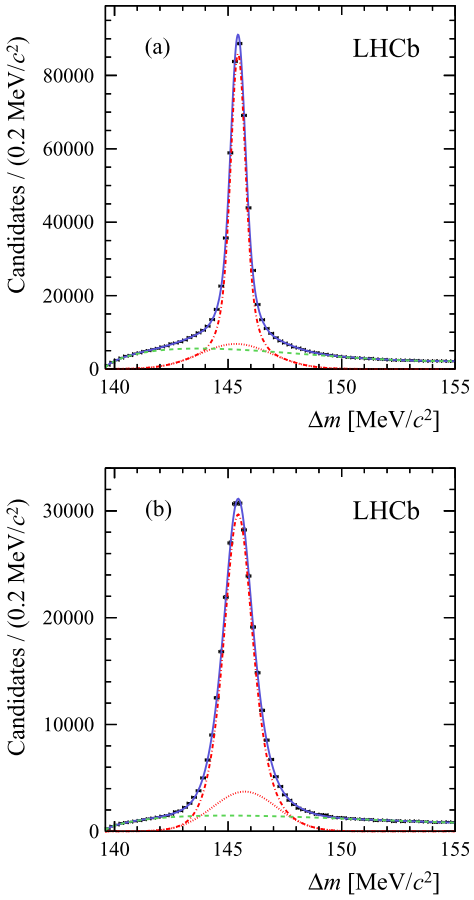

Fig. 1. Distribution of Δm with fit overlaid for the selected data set with (a) resolved and (b) merged π^0 candidates. The lines show the fit results for total signal (dot-dashed red), widest Gaussian signal component (dotted red), background (dashed green), and total (solid blue). (For interpretation of the references to colour in this figure legend, the reader is referred to the web version of this article.)

of 75–195 MeV/c^2. The purity of the merged π^0 sample is nevertheless significantly higher with respect to the resolved π^0, as it benefits from large transverse energy and much lower combinatorial background.

Cross-feed from $D^0 \to K^-\pi^+\pi^0$ decays, with a kaon misidentified as a pion, is reduced with requirements on the $\pi^\pm$ particle identification based on the ring-imaging Cherenkov detectors.

The D^0 candidates satisfying the above criteria and having invariant mass $m(\pi^-\pi^+\pi^0)$ within 40 (60) MeV/c^2 of the known D^0 mass are accepted in the resolved (merged) sample; this range corresponds to approximately four times the $m(\pi^-\pi^+\pi^0)$ resolution. The D^{*+} candidates, formed with the D^0 and π_s^+ candidate, have their entire decay chain refitted requiring that the D^{*+} candidate originates from the corresponding PV, and π^0 and D^0 candidates have their nominal masses. This improves the D^{*+} mass resolution and the resolution in the $D^0 \to \pi^-\pi^+\pi^0$ Dalitz plot, while a requirement put on the fit quality efficiently suppresses the background. This requirement also suppresses the contribution from the D^{*+} mesons originating from long-lived b-hadrons. The remainder of this component is not affected by CP asymmetries in b-hadrons since the flavour tag is obtained from the D^{*+} meson.

This preliminary selection is followed by a multivariate analysis based on a BDT. Signal and background samples used to train the BDT are obtained by applying the *sPlot* technique [12] to a quarter of the real data. The *sWeights* for signal and background separation are determined from a fit to the distribution of the mass difference, $\Delta m \equiv m(\pi^-\pi^+\pi^0\ \pi_s^+) - m(\pi^-\pi^+\pi^0)$, separately for the

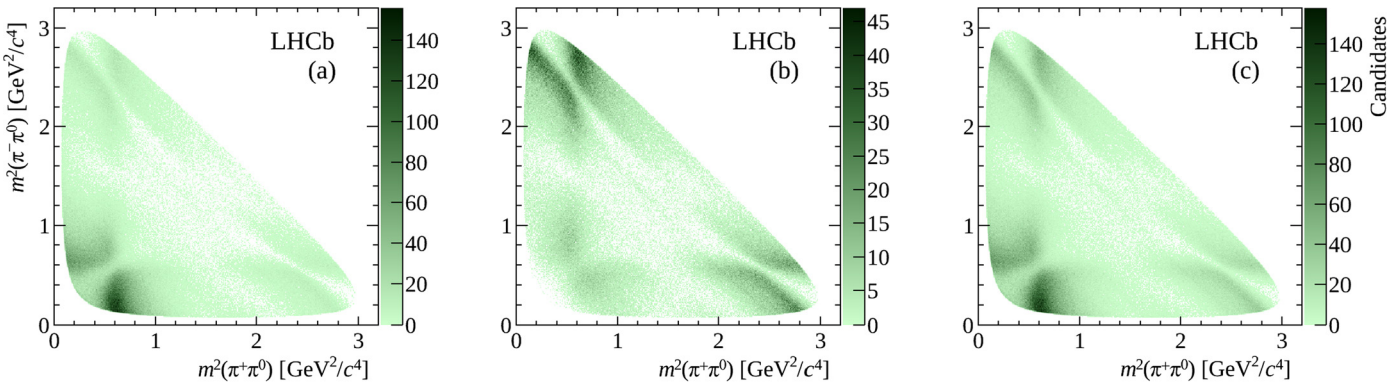

Fig. 2. Dalitz plot of the (a) resolved, (b) merged and (c) combined $D^0 \to \pi^-\pi^+\pi^0$ data sample. Enhanced event densities in the phase-space corners originate from the $\rho(770)$ resonances.

resolved and merged samples. The BDT uses the variables related to the kinematic and topological properties of the signal decays, as well as the π^0 quality. It is trained separately for the resolved and merged data categories. The most discriminating variables in the resolved sample are $p_T(\pi_s^+)$, $p_T(D^0)$ and $p_T(\pi^0)$, while in the merged sample these are $p_T(\pi_s^+)$, $p_T(D^0)$ and the D^0 χ^2_{IP}. The optimal value of the BDT discriminant is determined by estimating the D^{*+} signal significance for various requirements on the BDT output. It retains approximately 75% (90%) of the resolved (merged) signal events while removing 90% (55%) of the background. Fig. 1 shows the Δm distributions for the selected data set for events with resolved and merged π^0 candidates. The signal shapes, fitted in Fig. 1 with a sum of three Gaussian functions, significantly differ between both samples reflecting the different π^0 momentum resolutions. The lower momentum resolution of the merged π^0 mesons relative to the resolved π^0 mesons makes the core part of the merged signal distribution wider, while the low-p_T π^0 mesons contributing to the resolved signal enlarge its tail component. The background shape is fitted using a second-order polynomial multiplied by $\sqrt{1-m_{\pi^+}/\Delta m}$.

The final signal sample is selected requiring $|\Delta m - 145.4| < 1.8$ MeV/c^2, which corresponds to roughly four times the effective Δm resolution. The effective resolution is similar for both resolved and merged π^0 samples when averaging the narrow and broad components of the peak. This gives 416×10^3 resolved and 247×10^3 merged signal candidates with a purity of 82% and 91%, respectively. The Dalitz plot of the final signal sample is shown in Fig. 2. The smaller number of candidates in the low $m^2(\pi^+\pi^-)$ region compared with the high $m^2(\pi^+\pi^-)$ region is due to acceptance effects related to the π^0 reconstruction as discussed in Section 5.

4. Energy test method

Model-independent searches for local *CP* violation are typically carried out using a binned χ^2 approach to compare the relative density in the Dalitz plot of a decay and its *CP*-conjugate sample (see for example [5,13]). A model-independent unbinned statistical method called the energy test was introduced in Refs. [6,7]. Ref. [14] suggests applying this method to Dalitz plot analyses and demonstrates the potential to obtain improved sensitivity to *CP* violation over the standard binned approach. This Letter describes the first application of this technique to experimental data.

In this method a test statistic, T, is used to compare average distances in phase space, based on a metric function, ψ_{ij}, of pairs of events ij belonging to two samples of opposite flavour. It is defined as

$$T = \sum_{i,j>i}^{n} \frac{\psi_{ij}}{n(n-1)} + \sum_{i,j>i}^{\bar{n}} \frac{\psi_{ij}}{\bar{n}(\bar{n}-1)} - \sum_{i,j}^{n,\bar{n}} \frac{\psi_{ij}}{n\bar{n}}, \tag{1}$$

where the first and second terms correspond to a metric-weighted average distance of events within n events of one flavour and $\bar{n}$ events of the opposite flavour, respectively. The third term measures the weighted average distance of events in one flavour sample to events of the opposite flavour sample. The normalisation factors in the denominator remove the impact of global asymmetries. If the distributions of events in both flavour samples are identical, T will fluctuate around a value close to zero.

The metric function should be falling with increasing distance d_{ij} between events i and j, in order to increase the sensitivity to local asymmetries. A Gaussian metric is chosen, defined as $\psi_{ij} \equiv \psi(d_{ij}) = e^{-d_{ij}^2/2\sigma^2}$ with a tunable parameter σ, which describes the effective radius in phase space within which a local asymmetry is measured. Thus, this parameter should be larger than the resolution of d_{ij} and small enough not to dilute locally varying asymmetries.

The distance between two points in phase space is usually measured as the distance in the Dalitz plot. However, this distance depends on the choice of the axes of the Dalitz plot. This dependence is removed by using all three invariant masses to determine the distance, d_{ij}, calculated as the length of the displacement vector $\Delta\vec{x}_{ij} = (m^{2,j}_{12} - m^{2,i}_{12}, m^{2,j}_{23} - m^{2,i}_{23}, m^{2,j}_{13} - m^{2,i}_{13})$, where the $1,2,3$ subscripts indicate the final-state particles. Using all three invariant masses does not add information, but it avoids an arbitrary choice that could impact the sensitivity of the method to different *CP* violation scenarios.

In the case of *CP* violation, the average distances entering in the third term of Eq. (1) are larger, which, because of the characteristics of the metric function, leads to a reduced magnitude of this term. Therefore larger *CP* asymmetries lead to larger values of T. This is translated into a p-value under the hypothesis of *CP* symmetry by comparing the nominal T value observed in data to a distribution of T values obtained from permutation samples, where the flavour of each candidate is randomly reassigned to simulate samples without *CP* violation. The p-value for the no *CP* violation hypothesis is obtained as the fraction of permutation T values greater than the nominal T value.

A statistical uncertainty of the p-value is obtained as a binomial standard deviation. If large *CP* violation is observed, the observed T value is likely to lie outside the range of permutation T values. In this case the permutation T distribution can be fitted with a generalised extreme value (GEV) function, as demonstrated in Refs. [6,7] and verified in large simulation samples for this analysis. The GEV function is defined as

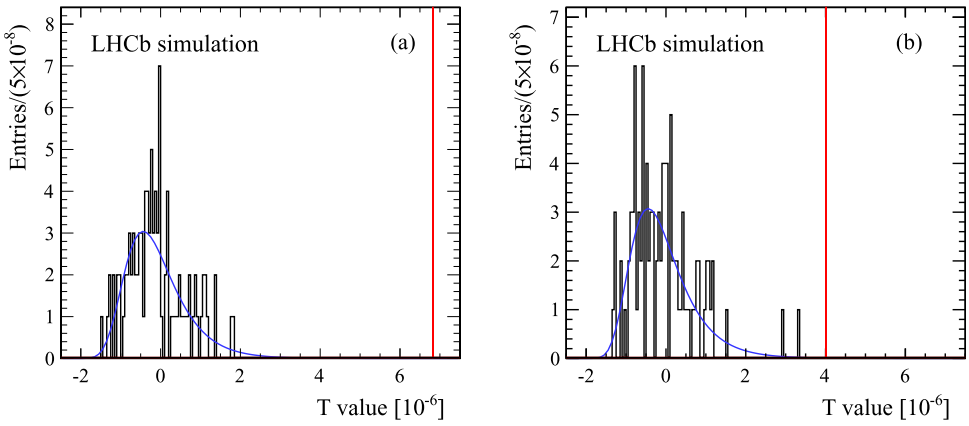

Fig. 3. Distribution of permutation T values fitted with a GEV function for the simulated sample and showing the nominal T value as a vertical line for (a) 2% *CP* violation in the amplitude and (b) 1° phase *CP* violation of the ρ^+ resonance.

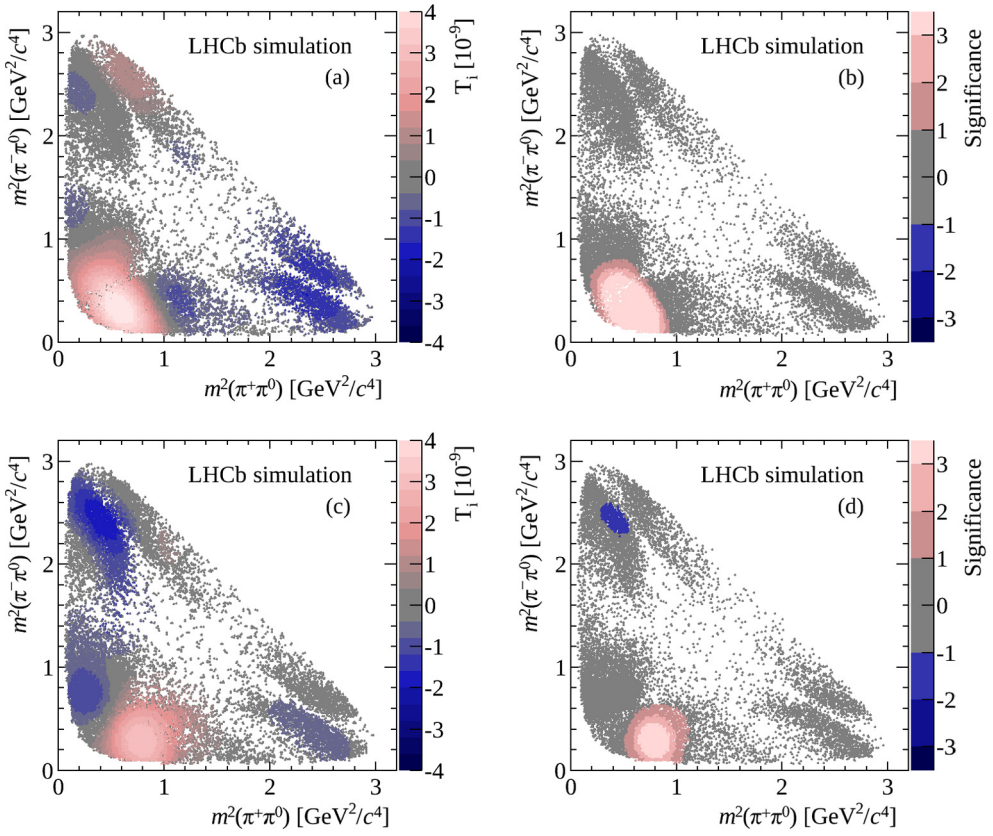

Fig. 4. (a), (c) T_i value distributions, and (b), (d) local asymmetry significances for (top) 2% *CP* violation in the amplitude and (bottom) 1° phase *CP* violation of the ρ^+ resonance.

$$f(T;\mu,\delta,\xi) = N\left[1+\xi\left(\frac{T-\mu}{\delta}\right)\right]^{(-1/\xi)-1} \times \exp\left\{-\left[1+\xi\left(\frac{T-\mu}{\delta}\right)\right]^{-1/\xi}\right\}, \quad (2)$$

with normalisation N, location parameter μ, scale parameter δ, and shape parameter ξ. This function is set to zero for $T > \mu - \delta/\xi$ for $\xi > 0$, and for $T < \mu - \delta/\xi$ for $\xi < 0$. Fig. 3 shows an example T value distribution with a GEV function fit for a simulated data set including *CP* violation (see Section 5).

The p-value from the fitted T distribution can be calculated as the fraction of the integral of the function above the nominal T value. The uncertainty on the p-value is obtained by randomly re-sampling the fit parameters within their uncertainties, taking into account their correlations, and by extracting a p-value for each of these generated T distributions. The spread of the resulting p-value distribution is used to set 68% confidence uncertainties. A 90% confidence upper limit is quoted where no significantly non-zero p-value can be obtained from the fit.

The number of available permutations is constrained by the available computing time. The default p-value extraction uses the counting method as long as at least three permutation T values are found to be larger than the observed T value. Beyond that, the p-value is extracted by integrating the fitted GEV function. The p-values presented here are based on 1000 permutations for the

default data results and on 100 permutations for the sensitivity studies.

A visualisation of regions of significant asymmetry is obtained by assigning an asymmetry significance to each event. The contributions of a single event of one flavour, T_i, and a single event of the opposite flavour, $\overline{T}_i$, to the total T value are given by

$$T_i = \frac{1}{2n(n-1)}\sum_{j\neq i}^{n}\psi_{ij} - \frac{1}{2n\bar{n}}\sum_{j}^{\bar{n}}\psi_{ij},$$
$$\overline{T}_i = \frac{1}{2\bar{n}(\bar{n}-1)}\sum_{j\neq i}^{\bar{n}}\psi_{ij} - \frac{1}{2n\bar{n}}\sum_{j}^{n}\psi_{ij}. \quad (3)$$

Example T_i distributions for the simulated CP violating data sets are shown in Fig. 4(a), (c); events contributing with T_i of the largest magnitude point to CP violation regions. However, the CP asymmetry arising from the ρ^+ amplitude difference (Fig. 4(a)) produces a global asymmetry, $n > \bar{n}$. Through the normalisation factors in Eq. (3), this leads to negative T_i regions for approximately $m^2(\pi^+\pi^0) > 2$ GeV$^2/c^4$, where the numbers of D^0 and $\overline{D}^0$ mesons are equal.

Having obtained the T_i and $\overline{T}_i$ values for all events, a permutation method is also used here to define the level of significance. The distributions of the smallest negative and largest positive T_i values of each permutation, $T_i^{\min}$ and $T_i^{\max}$, are used to assign significances of negative and positive asymmetries, respectively. Positive (negative) local asymmetry significances are T_i values greater (smaller) than the fraction of the $T_i^{\max}$ ($T_i^{\min}$) distribution that corresponds to the significance level. The same procedure is applied to the $\overline{T}_i$ distribution, leading to a Dalitz plot with an inverted asymmetry pattern.

The asymmetry significances for each simulated event are plotted on a Dalitz plot (see Fig. 4(b), (d)). If an amplitude difference exists between CP-conjugate states of a resonance, the region of significant asymmetry appears as a band around the mass of the resonance on the plot. If a phase difference is present instead, regions of positive and negative asymmetry appear around the resonance on the plot, indicating the phase shift.

The practical limitation of this method is that the number of mathematical operations scales quadratically with the sample size. Furthermore, a significant number of permutations is required to get a sufficient precision on the p-value. In this analysis the method is implemented using parallelisation on graphics processing units (GPUs) [15].

5. Sensitivity studies

The interpretation of the results requires a study of the sensitivity of the present data sample to different types of CP violation. The sensitivity is examined based on simplified Monte Carlo samples generated according to the model described in Ref. [3] using the generator package Laura++ [16].

The selection efficiency has to be taken into account in these studies as it varies strongly across phase space. This efficiency is measured using a sample of events based on the full LHCb detector simulation. In the simulation, pp collisions are generated using Pythia [17,18] with a specific LHCb configuration [19]. Decays of hadronic particles are described by EvtGen [20], in which final-state radiation is generated using Photos [21]. The interaction of the generated particles with the detector and its response are implemented using the Geant4 toolkit [22,23] as described in Ref. [24]. The efficiency is shown to vary as a function of the $\pi^+\pi^-$ invariant mass, while it is found to be constant with respect to other variables. The resulting efficiency curves for merged and resolved π^0 mesons as well as for the combined sample are shown in Fig. 5. The small $m(\pi^+\pi^-)$ range corresponds to π^0 candidates with high momentum and is primarily covered by the merged π^0 sample. The overall efficiency in this region is low as the integrated merged π^0 identification efficiency is lower than for the resolved sample and decreases after its turn-on as the π^0 momentum increases. This affects in particular the ρ^0 resonance, as it lies entirely within the low acceptance region.

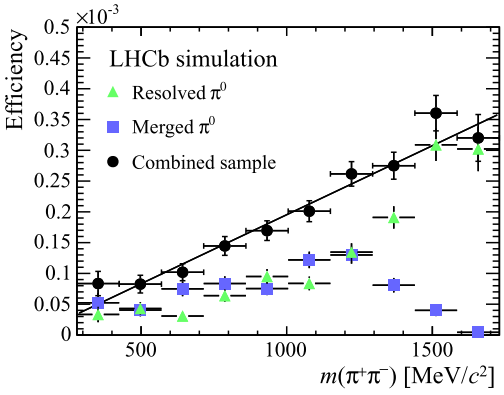

Fig. 5. The selection efficiency as a function of $m(\pi^+\pi^-)$. The efficiency for the combined sample is fitted with a straight line.

Table 1
Overview of sensitivities to various CP violation scenarios. ΔA and $\Delta\phi$ denote, respectively, change in amplitude and phase of the resonance R.

R (ΔA, $\Delta\phi$)	p-value (fit)	Upper limit
ρ^0 (4%, 0°)	$3.3^{+1.1}_{-3.3} \times 10^{-4}$	4.6×10^{-4}
ρ^0 (0%, 3°)	$1.5^{+1.7}_{-1.4} \times 10^{-3}$	3.8×10^{-3}
ρ^+ (2%, 0°)	$5.0^{+8.8}_{-3.8} \times 10^{-6}$	1.8×10^{-5}
ρ^+ (0%, 1°)	$6.3^{+5.5}_{-3.3} \times 10^{-4}$	1.4×10^{-3}
ρ^- (2%, 0°)	$2.0^{+1.3}_{-0.9} \times 10^{-3}$	3.9×10^{-3}
ρ^- (0%, 1.5°)	$8.9^{+22}_{-6.7} \times 10^{-7}$	4.2×10^{-6}

For further studies, the efficiency, based on the fitted curve, is then applied to simplified Monte Carlo data sets by randomly discarding events based on the candidate's position in phase space. Background events are simulated by resampling phase-space distributions extracted from Δm sideband regions. Inclusion of the background does not significantly reduce the sensitivity to the CP violation scenarios discussed below. This is due to the low level of background and due to it being CP symmetric within the present sensitivity.

Various CP asymmetries are introduced by modifying, for a chosen D^0 flavour, either the amplitude or the phase of one of the three intermediate ρ resonances dominating the $\pi^-\pi^+\pi^0$ phase space. The resulting sensitivities are shown in Table 1. The p-values, including their statistical uncertainties, are obtained from fits of GEV functions to the T value distributions and 90% confidence limits are given in addition.

The sensitivity is comparable to that of the BaBar analysis [5] for the ρ^0 resonance and significantly better for the ρ^+ and ρ^- resonances. This is expected due to the variation of the selection efficiency across phase space, which disfavours the ρ^0 region.

The sensitivity of the method also depends on the choice of the metric parameter σ. Studies indicate good stability of the measured sensitivity for values of σ between 0.2 and 0.5 GeV$^2/c^4$, which are well above the resolution of the d_{ij} and small compared to the size of the phase space. The value $\sigma = 0.3$ GeV$^2/c^4$ yields the best sensitivity to some of the CP violation scenarios studied and was chosen, prior to the data unblinding, as the default value.

The optimal σ value may vary with different *CP* violation scenarios. Hence the final results are also quoted for several values of σ.

The standard binned method [13] is also applied to the simulated data sets. This study shows that the energy test provides results compatible with, and equally or more precise than the binned method.

There are two main sources of asymmetry that may degrade or bias the results. One is an asymmetry that may arise from background events and the other is due to particle detection asymmetries that could vary across phase space.

Background asymmetries are tested by applying the energy test to events in the upper Δm sideband, $\Delta m > 150$ MeV/c^2. No significant asymmetry is found. In addition, simplified simulation data sets are produced by generating signal candidates without *CP* violation and background candidates according to background distributions in data, separately for D^0 and $\overline{D}^0$ candidates and thus allowing for a background-induced asymmetry. These samples show a distribution of p-values consistent with the absence of any asymmetry. Further tests using a binned approach [13] confirm this conclusion. These are carried out on the Δm sideband data sample as well as on background samples obtained using the *sPlot* technique based on the Δm fits in Fig. 1. Both approaches show no indication of a background asymmetry. As the background present in the signal region is found to be *CP* symmetric, it is simply included in the T value calculation discussed in Section 4.

Local asymmetries are expected to arise, at a level below the current sensitivity, due to the momentum dependence of π^+/π^- detection asymmetries in combination with the different kinematic distributions of π^+ and π^- in certain regions of phase space.

These effects are tested using the Cabibbo-favoured decay $D^0 \to K^-\pi^+\pi^0$ as a control mode. This channel is affected by kaon detection asymmetries, which are known to be larger than pion detection asymmetries and thus should serve as a conservative test. The data sample is split into eight subsets, each of which contains approximately the same amount of data as the signal sample. The energy test yields p-values between 3% and 74%, which is consistent with the assumption that detection asymmetries are below the current level of sensitivity. A further test is conducted by splitting the control mode data sample by the polarity of the spectrometer dipole magnet, which yields two large approximately equal-sized samples. The resulting p-values of 8% and 15% show no evidence of sizable biases due to detector asymmetries.

6. Results and conclusions

The application of the energy test to all selected $D^0 \to \pi^-\pi^+\pi^0$ candidates using a metric parameter of $\sigma = 0.3$ GeV$^2/c^4$ yields $T = 1.84 \times 10^{-6}$. The permutation T value distribution is shown in Fig. 6(a). By counting the fraction of permutations with a T value above the nominal T value in the data, a p-value of $(2.6 \pm 0.5) \times 10^{-2}$ is extracted. Alternatively, extrapolation from a fit to the GEV function gives a p-value of $(2.1 \pm 0.3) \times 10^{-2}$. The significance levels of the T_i values are shown in Fig. 6(b). A small phase-space region dominated by the ρ^+ resonance contains candidates with a local positive asymmetry exceeding 1σ significance. Varying the metric parameter results in the p-values listed in Table 2; all the p-values are at the 10^{-2} level.

The data sample has been split according to various criteria to test the stability of the results. Analyses of sub-samples with opposite magnet polarity, with different trigger configurations, and with fiducial selection requirements removing areas of high local asymmetry of the tagging soft pion from the D^{*+} decay all show good consistency of the results.

Table 2
Results for various metric parameter values. The p-values are obtained with the counting method.

σ [GeV$^2/c^4$]	p-value
0.2	$(4.6 \pm 0.6) \times 10^{-2}$
0.3	$(2.6 \pm 0.5) \times 10^{-2}$
0.4	$(1.7 \pm 0.4) \times 10^{-2}$
0.5	$(2.1 \pm 0.5) \times 10^{-2}$

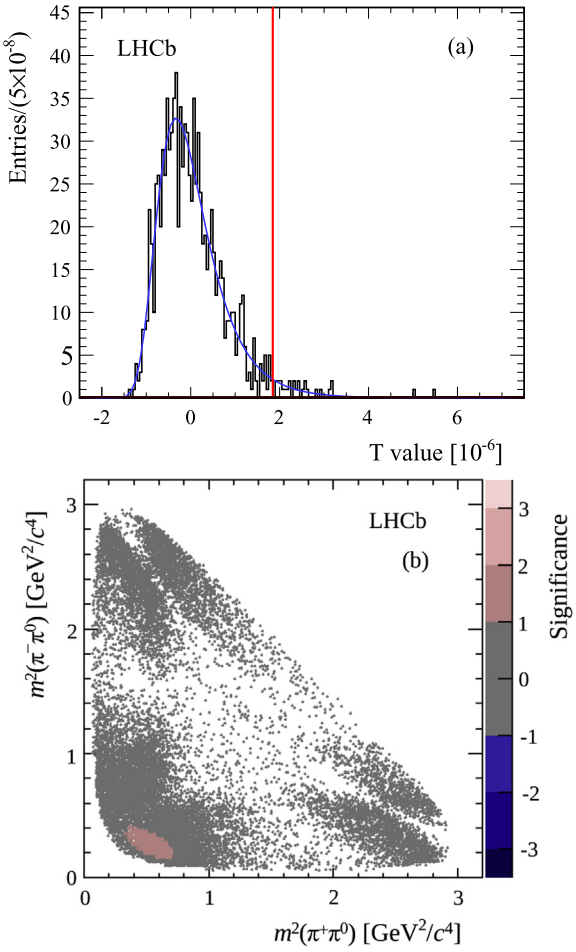

Fig. 6. (a) Permutation T value distribution showing the fit function and the measured T value as a red line. (b) Visualisation of local asymmetry significances. The positive (negative) asymmetry significance is set for the D^0 candidates having positive (negative) contribution to the measured T value, respectively (see Section 4). (For interpretation of the references to colour in this figure legend, the reader is referred to the web version of this article.)

In summary, a search for time-integrated *CP* violation in the Cabibbo-suppressed decay $D^0 \to \pi^-\pi^+\pi^0$ is performed using a novel unbinned model-independent technique. The analysis has the best sensitivity from a single experiment to *CP* violation in this decay. The data are found to be consistent with the hypothesis of *CP* symmetry with a p-value of (2.6 ± 0.5)%.

Acknowledgements

We express our gratitude to our colleagues in the CERN accelerator departments for the excellent performance of the LHC. We thank the technical and administrative staff at the LHCb institutes. We acknowledge support from CERN and from the national agencies: CAPES, CNPq, FAPERJ and FINEP (Brazil); NSFC (China); CNRS/IN2P3 (France); BMBF, DFG, HGF and MPG (Germany); SFI

(Ireland); INFN (Italy); FOM and NWO (The Netherlands); MNiSW and NCN (Poland); MEN/IFA (Romania); MinES and FANO (Russia); MinECo (Spain); SNSF and SER (Switzerland); NASU (Ukraine); STFC (United Kingdom); NSF (USA). The Tier1 computing centres are supported by IN2P3 (France), KIT and BMBF (Germany), INFN (Italy), NWO and SURF (The Netherlands), PIC (Spain), GridPP (United Kingdom). This work was supported in part by an allocation of computing time from the Ohio Supercomputer Center. We are indebted to the communities behind the multiple open source software packages on which we depend. We are also thankful for the computing resources and the access to software R&D tools provided by Yandex LLC (Russia). Individual groups or members have received support from EPLANET, Marie Skłodowska-Curie Actions and ERC (European Union), Conseil général de Haute-Savoie, Labex ENIGMASS and OCEVU, Région Auvergne (France), RFBR (Russia), XuntaGal and GENCAT (Spain), Royal Society and Royal Commission for the Exhibition of 1851 (United Kingdom).

References

[1] Y. Grossman, A.L. Kagan, Y. Nir, New physics and *CP* violation in singly Cabibbo suppressed *D* decays, Phys. Rev. D 75 (2007) 036008, arXiv:hep-ph/0609178.
[2] LHCb Collaboration, R. Aaij, et al., Measurements of indirect *CP* asymmetries in $D^0 \to K^-K^+$ and $D^0 \to \pi^-\pi^+$ decays, Phys. Rev. Lett. 112 (2014) 041801, arXiv:1310.7201.
[3] BaBar Collaboration, B. Aubert, et al., Measurement of *CP* violation parameters with a Dalitz plot analysis of $B^\pm \to D(\pi^+\pi^-\pi^0)K^\pm$, Phys. Rev. Lett. 99 (2007) 251801, arXiv:hep-ex/0703037.
[4] Y. Grossman, A.L. Kagan, J. Zupan, Testing for new physics in singly Cabibbo suppressed *D* decays, Phys. Rev. D 85 (2012) 114036, arXiv:1204.3557.
[5] BaBar Collaboration, B. Aubert, et al., Search for *CP* Violation in neutral *D* meson Cabibbo-suppressed three-body decays, Phys. Rev. D 78 (2008) 051102, arXiv:0802.4035.
[6] B. Aslan, G. Zech, New test for the multivariate two-sample problem based on the concept of minimum energy, J. Stat. Comput. Simul. 75 (2005) 109.
[7] B. Aslan, G. Zech, Statistical energy as a tool for binning-free, multivariate goodness-of-fit tests, two-sample comparison and unfolding, Nucl. Instrum. Methods A 537 (2005) 626.
[8] LHCb Collaboration, A.A. Alves Jr., et al., The LHCb detector at the LHC, J. Instrum. 3 (2008) S08005.
[9] R. Aaij, et al., LHCb detector performance, LHCb-DP-2014-002, in preparation.
[10] L. Breiman, J.H. Friedman, R.A. Olshen, C.J. Stone, Classification and Regression Trees, Wadsworth International Group, Belmont, CA, USA, 1984.
[11] R.E. Schapire, Y. Freund, A decision-theoretic generalization of on-line learning and an application to boosting, J. Comput. Syst. Sci. 55 (1997) 119.
[12] M. Pivk, F.R. Le, Diberder, sPlot: a statistical tool to unfold data distributions, Nucl. Instrum. Methods A 555 (2005) 356, arXiv:physics/0402083.
[13] I. Bediaga, et al., On a *CP* anisotropy measurement in the Dalitz plot, Phys. Rev. D 80 (2009) 096006, arXiv:0905.4233.
[14] M. Williams, Observing *CP* violation in many-body decays, Phys. Rev. D 84 (2011) 054015, arXiv:1105.5338.
[15] NVIDIA Corporation, Thrust quick start guide, 2014, DU-06716-001.
[16] T. Latham, et al., `Laura++` Dalitz plot fitting package, http://laura.hepforge.org/.
[17] T. Sjöstrand, S. Mrenna, P. Skands, PYTHIA 6.4 physics and manual, JHEP 05 (2006) 026, arXiv:hep-ph/0603175.
[18] T. Sjöstrand, S. Mrenna, P. Skands, A brief introduction to PYTHIA 8.1, Comput. Phys. Commun. 178 (2008) 852, arXiv:0710.3820.
[19] I. Belyaev, et al., Handling of the generation of primary events in Gauss, the LHCb simulation framework, Nuclear Science Symposium Conference Record (NSS/MIC) IEEE (2010) 1155.
[20] D.J. Lange, The EvtGen particle decay simulation package, Nucl. Instrum. Methods A 462 (2001) 152.
[21] P. Golonka, Z. Was, PHOTOS Monte Carlo: a precision tool for QED corrections in *Z* and *W* decays, Eur. Phys. J. C 45 (2006) 97, arXiv:hep-ph/0506026.
[22] Geant4 Collaboration, J. Allison, et al., Geant4 developments and applications, IEEE Trans. Nucl. Sci. 53 (2006) 270.
[23] Geant4 Collaboration, S. Agostinelli, et al., Geant4: a simulation toolkit, Nucl. Instrum. Methods A 506 (2003) 250.
[24] M. Clemencic, et al., The LHCb simulation application, Gauss: design, evolution and experience, J. Phys. Conf. Ser. 331 (2011) 032023.

LHCb Collaboration

R. Aaij [41], B. Adeva [37], M. Adinolfi [46], A. Affolder [52], Z. Ajaltouni [5], S. Akar [6], J. Albrecht [9], F. Alessio [38], M. Alexander [51], S. Ali [41], G. Alkhazov [30], P. Alvarez Cartelle [37], A.A. Alves Jr [25,38], S. Amato [2], S. Amerio [22], Y. Amhis [7], L. An [3], L. Anderlini [17,g], J. Anderson [40], R. Andreassen [57], M. Andreotti [16,f], J.E. Andrews [58], R.B. Appleby [54], O. Aquines Gutierrez [10], F. Archilli [38], A. Artamonov [35], M. Artuso [59], E. Aslanides [6], G. Auriemma [25,n], M. Baalouch [5], S. Bachmann [11], J.J. Back [48], A. Badalov [36], C. Baesso [60], W. Baldini [16], R.J. Barlow [54], C. Barschel [38], S. Barsuk [7], W. Barter [47], V. Batozskaya [28], V. Battista [39], A. Bay [39], L. Beaucourt [4], J. Beddow [51], F. Bedeschi [23], I. Bediaga [1], S. Belogurov [31], K. Belous [35], I. Belyaev [31], E. Ben-Haim [8], G. Bencivenni [18], S. Benson [38], J. Benton [46], A. Berezhnoy [32], R. Bernet [40], M.-O. Bettler [47], M. van Beuzekom [41], A. Bien [11], S. Bifani [45], T. Bird [54], A. Bizzeti [17,i], P.M. Bjørnstad [54], T. Blake [48], F. Blanc [39], J. Blouw [10], S. Blusk [59], V. Bocci [25], A. Bondar [34], N. Bondar [30,38], W. Bonivento [15,38], S. Borghi [54], A. Borgia [59], M. Borsato [7], T.J.V. Bowcock [52], E. Bowen [40], C. Bozzi [16], T. Brambach [9], D. Brett [54], M. Britsch [10], T. Britton [59], J. Brodzicka [54], N.H. Brook [46], H. Brown [52], A. Bursche [40], J. Buytaert [38], S. Cadeddu [15], R. Calabrese [16,f], M. Calvi [20,k], M. Calvo Gomez [36,p], P. Campana [18], D. Campora Perez [38], A. Carbone [14,d], G. Carboni [24,l], R. Cardinale [19,38,j], A. Cardini [15], L. Carson [50], K. Carvalho Akiba [2], G. Casse [52], L. Cassina [20,k], L. Castillo Garcia [38], M. Cattaneo [38], Ch. Cauet [9], R. Cenci [23], M. Charles [8], Ph. Charpentier [38], M. Chefdeville [4], S. Chen [54], S.-F. Cheung [55], N. Chiapolini [40], M. Chrzaszcz [40,26], X. Cid Vidal [38], G. Ciezarek [41], P.E.L. Clarke [50], M. Clemencic [38], H.V. Cliff [47], J. Closier [38], V. Coco [38], J. Cogan [6], E. Cogneras [5], V. Cogoni [15], L. Cojocariu [29], G. Collazuol [22], P. Collins [38], A. Comerma-Montells [11], A. Contu [15,38], A. Cook [46], M. Coombes [46], S. Coquereau [8], G. Corti [38], M. Corvo [16,f], I. Counts [56], B. Couturier [38], G.A. Cowan [50], D.C. Craik [48], A.C. Crocombe [48], M. Cruz Torres [60], S. Cunliffe [53], R. Currie [53], C. D'Ambrosio [38], J. Dalseno [46], P. David [8], P.N.Y. David [41], A. Davis [57], K. De Bruyn [41], S. De Capua [54], M. De Cian [11], J.M. De Miranda [1], L. De Paula [2], W. De Silva [57], P. De Simone [18], C.-T. Dean [51], D. Decamp [4], M. Deckenhoff [9], L. Del Buono [8], N. Déléage [4], D. Derkach [55],

O. Deschamps [5], F. Dettori [38], A. Di Canto [38], H. Dijkstra [38], S. Donleavy [52], F. Dordei [11], M. Dorigo [39], A. Dosil Suárez [37], D. Dossett [48], A. Dovbnya [43], K. Dreimanis [52], G. Dujany [54], F. Dupertuis [39], P. Durante [38], R. Dzhelyadin [35], A. Dziurda [26], A. Dzyuba [30], S. Easo [49,38], U. Egede [53], V. Egorychev [31], S. Eidelman [34], S. Eisenhardt [50], U. Eitschberger [9], R. Ekelhof [9], L. Eklund [51], I. El Rifai [5], Ch. Elsasser [40], S. Ely [59], S. Esen [11], H.-M. Evans [47], T. Evans [55], A. Falabella [14], C. Färber [11], C. Farinelli [41], N. Farley [45], S. Farry [52], R. Fay [52], D. Ferguson [50], V. Fernandez Albor [37], F. Ferreira Rodrigues [1], M. Ferro-Luzzi [38], S. Filippov [33], M. Fiore [16,f], M. Fiorini [16,f], M. Firlej [27], C. Fitzpatrick [39], T. Fiutowski [27], P. Fol [53], M. Fontana [10], F. Fontanelli [19,j], R. Forty [38], O. Francisco [2], M. Frank [38], C. Frei [38], M. Frosini [17,g], J. Fu [21,38], E. Furfaro [24,l], A. Gallas Torreira [37], D. Galli [14,d], S. Gallorini [22,38], S. Gambetta [19,j], M. Gandelman [2], P. Gandini [59], Y. Gao [3], J. García Pardiñas [37], J. Garofoli [59], J. Garra Tico [47], L. Garrido [36], D. Gascon [36], C. Gaspar [38], R. Gauld [55], L. Gavardi [9], A. Geraci [21,v], E. Gersabeck [11], M. Gersabeck [54,*], T. Gershon [48], Ph. Ghez [4], A. Gianelle [22], S. Gianì [39], V. Gibson [47], L. Giubega [29], V.V. Gligorov [38], C. Göbel [60], D. Golubkov [31], A. Golutvin [53,31,38], A. Gomes [1,a], C. Gotti [20,k], M. Grabalosa Gándara [5], R. Graciani Diaz [36], L.A. Granado Cardoso [38], E. Graugés [36], E. Graverini [40], G. Graziani [17], A. Grecu [29], E. Greening [55], S. Gregson [47], P. Griffith [45], L. Grillo [11], O. Grünberg [63], B. Gui [59], E. Gushchin [33], Yu. Guz [35,38], T. Gys [38], C. Hadjivasiliou [59], G. Haefeli [39], C. Haen [38], S.C. Haines [47], S. Hall [53], B. Hamilton [58], T. Hampson [46], X. Han [11], S. Hansmann-Menzemer [11], N. Harnew [55], S.T. Harnew [46], J. Harrison [54], J. He [38], T. Head [38], V. Heijne [41], K. Hennessy [52], P. Henrard [5], L. Henry [8], J.A. Hernando Morata [37], E. van Herwijnen [38], M. Heß [63], A. Hicheur [2], D. Hill [55], M. Hoballah [5], C. Hombach [54], W. Hulsbergen [41], P. Hunt [55], N. Hussain [55], D. Hutchcroft [52], D. Hynds [51], M. Idzik [27], P. Ilten [56], R. Jacobsson [38], A. Jaeger [11], J. Jalocha [55], E. Jans [41], P. Jaton [39], A. Jawahery [58], F. Jing [3], M. John [55], D. Johnson [38], C.R. Jones [47], C. Joram [38], B. Jost [38], N. Jurik [59], S. Kandybei [43], W. Kanso [6], M. Karacson [38], T.M. Karbach [38], S. Karodia [51], M. Kelsey [59], I.R. Kenyon [45], T. Ketel [42], B. Khanji [20,38,k], C. Khurewathanakul [39], S. Klaver [54], K. Klimaszewski [28], O. Kochebina [7], M. Kolpin [11], I. Komarov [39], R.F. Koopman [42], P. Koppenburg [41,38], M. Korolev [32], A. Kozlinskiy [41], L. Kravchuk [33], K. Kreplin [11], M. Kreps [48], G. Krocker [11], P. Krokovny [34], F. Kruse [9], W. Kucewicz [26,o], M. Kucharczyk [20,26,k], V. Kudryavtsev [34], K. Kurek [28], T. Kvaratskheliya [31], V.N. La Thi [39], D. Lacarrere [38], G. Lafferty [54], A. Lai [15], D. Lambert [50], R.W. Lambert [42], G. Lanfranchi [18], C. Langenbruch [48], B. Langhans [38], T. Latham [48], C. Lazzeroni [45], R. Le Gac [6], J. van Leerdam [41], J.-P. Lees [4], R. Lefèvre [5], A. Leflat [32], J. Lefrançois [7], S. Leo [23], O. Leroy [6], T. Lesiak [26], B. Leverington [11], Y. Li [3], T. Likhomanenko [64], M. Liles [52], R. Lindner [38], C. Linn [38], F. Lionetto [40], B. Liu [15], S. Lohn [38], I. Longstaff [51], J.H. Lopes [2], N. Lopez-March [39], P. Lowdon [40], D. Lucchesi [22,r], H. Luo [50], A. Lupato [22], E. Luppi [16,f], O. Lupton [55], F. Machefert [7], I.V. Machikhiliyan [31], F. Maciuc [29], O. Maev [30], K. Maguire [54], S. Malde [55], A. Malinin [64], G. Manca [15,e], G. Mancinelli [6], A. Mapelli [38], J. Maratas [5], J.F. Marchand [4], U. Marconi [14], C. Marin Benito [36], P. Marino [23,t], R. Märki [39], J. Marks [11], G. Martellotti [25], A. Martín Sánchez [7], M. Martinelli [39], D. Martinez Santos [42,38], F. Martinez Vidal [65], D. Martins Tostes [2], A. Massafferri [1], R. Matev [38], Z. Mathe [38], C. Matteuzzi [20], B. Maurin [39], A. Mazurov [45], M. McCann [53], J. McCarthy [45], A. McNab [54], R. McNulty [12], B. McSkelly [52], B. Meadows [57], F. Meier [9], M. Meissner [11], M. Merk [41], D.A. Milanes [62], M.-N. Minard [4], N. Moggi [14], J. Molina Rodriguez [60], S. Monteil [5], M. Morandin [22], P. Morawski [27], A. Mordà [6], M.J. Morello [23,t], J. Moron [27], A.-B. Morris [50], R. Mountain [59], F. Muheim [50], K. Müller [40], M. Mussini [14], B. Muster [39], P. Naik [46], T. Nakada [39], R. Nandakumar [49], I. Nasteva [2], M. Needham [50], N. Neri [21], S. Neubert [38], N. Neufeld [38], M. Neuner [11], A.D. Nguyen [39], T.D. Nguyen [39], C. Nguyen-Mau [39,q], M. Nicol [7], V. Niess [5], R. Niet [9], N. Nikitin [32], T. Nikodem [11], A. Novoselov [35], D.P. O'Hanlon [48], A. Oblakowska-Mucha [27,38], V. Obraztsov [35], S. Oggero [41], S. Ogilvy [51], O. Okhrimenko [44], R. Oldeman [15,e], C.J.G. Onderwater [66], M. Orlandea [29], J.M. Otalora Goicochea [2], A. Otto [38], P. Owen [53], A. Oyanguren [65], B.K. Pal [59], A. Palano [13,c], F. Palombo [21,u], M. Palutan [18], J. Panman [38], A. Papanestis [49,38], M. Pappagallo [51], L.L. Pappalardo [16,f], C. Parkes [54], C.J. Parkinson [9,45], G. Passaleva [17], G.D. Patel [52], M. Patel [53], C. Patrignani [19,j], A. Pearce [54], A. Pellegrino [41], M. Pepe Altarelli [38], S. Perazzini [14,d], P. Perret [5], M. Perrin-Terrin [6], L. Pescatore [45], E. Pesen [67], K. Petridis [53], A. Petrolini [19,j], E. Picatoste Olloqui [36], B. Pietrzyk [4], T. Pilař [48], D. Pinci [25], A. Pistone [19], S. Playfer [50], M. Plo Casasus [37], F. Polci [8], A. Poluektov [48,34], I. Polyakov [31], E. Polycarpo [2], A. Popov [35], D. Popov [10], B. Popovici [29], C. Potterat [2], E. Price [46], J.D. Price [52], J. Prisciandaro [39], A. Pritchard [52], C. Prouve [46], V. Pugatch [44], A. Puig Navarro [39], G. Punzi [23,s], W. Qian [4], B. Rachwal [26], J.H. Rademacker [46], B. Rakotomiaramanana [39], M. Rama [18],

M.S. Rangel [2], I. Raniuk [43], N. Rauschmayr [38], G. Raven [42], F. Redi [53], S. Reichert [54], M.M. Reid [48], A.C. dos Reis [1], S. Ricciardi [49], S. Richards [46], M. Rihl [38], K. Rinnert [52], V. Rives Molina [36], P. Robbe [7], A.B. Rodrigues [1], E. Rodrigues [54], P. Rodriguez Perez [54], S. Roiser [38], V. Romanovsky [35], A. Romero Vidal [37], M. Rotondo [22], J. Rouvinet [39], T. Ruf [38], H. Ruiz [36], P. Ruiz Valls [65], J.J. Saborido Silva [37], N. Sagidova [30], P. Sail [51], B. Saitta [15,e], V. Salustino Guimaraes [2], C. Sanchez Mayordomo [65], B. Sanmartin Sedes [37], R. Santacesaria [25], C. Santamarina Rios [37], E. Santovetti [24,l], A. Sarti [18,m], C. Satriano [25,n], A. Satta [24], D.M. Saunders [46], D. Savrina [31,32], M. Schiller [42], H. Schindler [38], M. Schlupp [9], M. Schmelling [10], B. Schmidt [38], O. Schneider [39], A. Schopper [38], M. Schubiger [39], M.-H. Schune [7], R. Schwemmer [38], B. Sciascia [18], A. Sciubba [25], A. Semennikov [31], I. Sepp [53], N. Serra [40], J. Serrano [6], L. Sestini [22], P. Seyfert [11], M. Shapkin [35], I. Shapoval [16,43,f], Y. Shcheglov [30], T. Shears [52], L. Shekhtman [34], V. Shevchenko [64], A. Shires [9], R. Silva Coutinho [48], G. Simi [22], M. Sirendi [47], N. Skidmore [46], I. Skillicorn [51], T. Skwarnicki [59], N.A. Smith [52], E. Smith [55,49], E. Smith [53], J. Smith [47], M. Smith [54], H. Snoek [41], M.D. Sokoloff [57], F.J.P. Soler [51], F. Soomro [39], D. Souza [46], B. Souza De Paula [2], B. Spaan [9], P. Spradlin [51], S. Sridharan [38], F. Stagni [38], M. Stahl [11], S. Stahl [11], O. Steinkamp [40], O. Stenyakin [35], S. Stevenson [55], S. Stoica [29], S. Stone [59], B. Storaci [40], S. Stracka [23], M. Straticiuc [29], U. Straumann [40], R. Stroili [22], V.K. Subbiah [38], L. Sun [57], W. Sutcliffe [53], K. Swientek [27], S. Swientek [9], V. Syropoulos [42], M. Szczekowski [28], P. Szczypka [39,38], T. Szumlak [27], S. T'Jampens [4], M. Teklishyn [7], G. Tellarini [16,f], F. Teubert [38], C. Thomas [55], E. Thomas [38], J. van Tilburg [41], V. Tisserand [4], M. Tobin [39], J. Todd [57], S. Tolk [42], L. Tomassetti [16,f], D. Tonelli [38], S. Topp-Joergensen [55], N. Torr [55], E. Tournefier [4], S. Tourneur [39], M.T. Tran [39], M. Tresch [40], A. Trisovic [38], A. Tsaregorodtsev [6], P. Tsopelas [41], N. Tuning [41], M. Ubeda Garcia [38], A. Ukleja [28], A. Ustyuzhanin [64], U. Uwer [11], C. Vacca [15], V. Vagnoni [14], G. Valenti [14], A. Vallier [7], R. Vazquez Gomez [18], P. Vazquez Regueiro [37], C. Vázquez Sierra [37], S. Vecchi [16], J.J. Velthuis [46], M. Veltri [17,h], G. Veneziano [39], M. Vesterinen [11], B. Viaud [7], D. Vieira [2], M. Vieites Diaz [37], X. Vilasis-Cardona [36,p], A. Vollhardt [40], D. Volyanskyy [10], D. Voong [46], A. Vorobyev [30], V. Vorobyev [34], C. Voß [63], J.A. de Vries [41], R. Waldi [63], C. Wallace [48], R. Wallace [12], J. Walsh [23], S. Wandernoth [11], J. Wang [59], D.R. Ward [47], N.K. Watson [45], D. Websdale [53], M. Whitehead [48], J. Wicht [38], D. Wiedner [11], G. Wilkinson [55,38], M. Wilkinson [59], M.P. Williams [45], M. Williams [56], H.W. Wilschut [66], F.F. Wilson [49], J. Wimberley [58], J. Wishahi [9], W. Wislicki [28], M. Witek [26], G. Wormser [7], S.A. Wotton [47], S. Wright [47], K. Wyllie [38], Y. Xie [61], Z. Xing [59], Z. Xu [39], Z. Yang [3], X. Yuan [3], O. Yushchenko [35], M. Zangoli [14], M. Zavertyaev [10,b], L. Zhang [59], W.C. Zhang [12], Y. Zhang [3], A. Zhelezov [11], A. Zhokhov [31], L. Zhong [3]

[1] *Centro Brasileiro de Pesquisas Físicas (CBPF), Rio de Janeiro, Brazil*
[2] *Universidade Federal do Rio de Janeiro (UFRJ), Rio de Janeiro, Brazil*
[3] *Center for High Energy Physics, Tsinghua University, Beijing, China*
[4] *LAPP, Université de Savoie, CNRS/IN2P3, Annecy-Le-Vieux, France*
[5] *Clermont Université, Université Blaise Pascal, CNRS/IN2P3, LPC, Clermont-Ferrand, France*
[6] *CPPM, Aix-Marseille Université, CNRS/IN2P3, Marseille, France*
[7] *LAL, Université Paris-Sud, CNRS/IN2P3, Orsay, France*
[8] *LPNHE, Université Pierre et Marie Curie, Université Paris Diderot, CNRS/IN2P3, Paris, France*
[9] *Fakultät Physik, Technische Universität Dortmund, Dortmund, Germany*
[10] *Max-Planck-Institut für Kernphysik (MPIK), Heidelberg, Germany*
[11] *Physikalisches Institut, Ruprecht-Karls-Universität Heidelberg, Heidelberg, Germany*
[12] *School of Physics, University College Dublin, Dublin, Ireland*
[13] *Sezione INFN di Bari, Bari, Italy*
[14] *Sezione INFN di Bologna, Bologna, Italy*
[15] *Sezione INFN di Cagliari, Cagliari, Italy*
[16] *Sezione INFN di Ferrara, Ferrara, Italy*
[17] *Sezione INFN di Firenze, Firenze, Italy*
[18] *Laboratori Nazionali dell'INFN di Frascati, Frascati, Italy*
[19] *Sezione INFN di Genova, Genova, Italy*
[20] *Sezione INFN di Milano Bicocca, Milano, Italy*
[21] *Sezione INFN di Milano, Milano, Italy*
[22] *Sezione INFN di Padova, Padova, Italy*
[23] *Sezione INFN di Pisa, Pisa, Italy*
[24] *Sezione INFN di Roma Tor Vergata, Roma, Italy*
[25] *Sezione INFN di Roma La Sapienza, Roma, Italy*
[26] *Henryk Niewodniczanski Institute of Nuclear Physics Polish Academy of Sciences, Kraków, Poland*
[27] *AGH – University of Science and Technology, Faculty of Physics and Applied Computer Science, Kraków, Poland*
[28] *National Center for Nuclear Research (NCBJ), Warsaw, Poland*
[29] *Horia Hulubei National Institute of Physics and Nuclear Engineering, Bucharest-Magurele, Romania*
[30] *Petersburg Nuclear Physics Institute (PNPI), Gatchina, Russia*
[31] *Institute of Theoretical and Experimental Physics (ITEP), Moscow, Russia*
[32] *Institute of Nuclear Physics, Moscow State University (SINP MSU), Moscow, Russia*
[33] *Institute for Nuclear Research of the Russian Academy of Sciences (INR RAN), Moscow, Russia*

[34] Budker Institute of Nuclear Physics (SB RAS) and Novosibirsk State University, Novosibirsk, Russia
[35] Institute for High Energy Physics (IHEP), Protvino, Russia
[36] Universitat de Barcelona, Barcelona, Spain
[37] Universidad de Santiago de Compostela, Santiago de Compostela, Spain
[38] European Organization for Nuclear Research (CERN), Geneva, Switzerland
[39] Ecole Polytechnique Fédérale de Lausanne (EPFL), Lausanne, Switzerland
[40] Physik-Institut, Universität Zürich, Zürich, Switzerland
[41] Nikhef National Institute for Subatomic Physics, Amsterdam, The Netherlands
[42] Nikhef National Institute for Subatomic Physics and VU University Amsterdam, Amsterdam, The Netherlands
[43] NSC Kharkiv Institute of Physics and Technology (NSC KIPT), Kharkiv, Ukraine
[44] Institute for Nuclear Research of the National Academy of Sciences (KINR), Kyiv, Ukraine
[45] University of Birmingham, Birmingham, United Kingdom
[46] H.H. Wills Physics Laboratory, University of Bristol, Bristol, United Kingdom
[47] Cavendish Laboratory, University of Cambridge, Cambridge, United Kingdom
[48] Department of Physics, University of Warwick, Coventry, United Kingdom
[49] STFC Rutherford Appleton Laboratory, Didcot, United Kingdom
[50] School of Physics and Astronomy, University of Edinburgh, Edinburgh, United Kingdom
[51] School of Physics and Astronomy, University of Glasgow, Glasgow, United Kingdom
[52] Oliver Lodge Laboratory, University of Liverpool, Liverpool, United Kingdom
[53] Imperial College London, London, United Kingdom
[54] School of Physics and Astronomy, University of Manchester, Manchester, United Kingdom
[55] Department of Physics, University of Oxford, Oxford, United Kingdom
[56] Massachusetts Institute of Technology, Cambridge, MA, United States
[57] University of Cincinnati, Cincinnati, OH, United States
[58] University of Maryland, College Park, MD, United States
[59] Syracuse University, Syracuse, NY, United States
[60] Pontifícia Universidade Católica do Rio de Janeiro (PUC-Rio), Rio de Janeiro, Brazil [w]
[61] Institute of Particle Physics, Central China Normal University, Wuhan, Hubei, China [x]
[62] Departamento de Fisica, Universidad Nacional de Colombia, Bogota, Colombia [y]
[63] Institut für Physik, Universität Rostock, Rostock, Germany [z]
[64] National Research Centre Kurchatov Institute, Moscow, Russia [aa]
[65] Instituto de Fisica Corpuscular (IFIC), Universitat de Valencia-CSIC, Valencia, Spain [ab]
[66] Van Swinderen Institute, University of Groningen, Groningen, The Netherlands [ac]
[67] Celal Bayar University, Manisa, Turkey [ad]

* Corresponding author.
E-mail address: marco.gersabeck@manchester.ac.uk (M. Gersabeck).
[a] Universidade Federal do Triângulo Mineiro (UFTM), Uberaba-MG, Brazil.
[b] P.N. Lebedev Physical Institute, Russian Academy of Science (LPI RAS), Moscow, Russia.
[c] Università di Bari, Bari, Italy.
[d] Università di Bologna, Bologna, Italy.
[e] Università di Cagliari, Cagliari, Italy.
[f] Università di Ferrara, Ferrara, Italy.
[g] Università di Firenze, Firenze, Italy.
[h] Università di Urbino, Urbino, Italy.
[i] Università di Modena e Reggio Emilia, Modena, Italy.
[j] Università di Genova, Genova, Italy.
[k] Università di Milano Bicocca, Milano, Italy.
[l] Università di Roma Tor Vergata, Roma, Italy.
[m] Università di Roma La Sapienza, Roma, Italy.
[n] Università della Basilicata, Potenza, Italy.
[o] AGH – University of Science and Technology, Faculty of Computer Science, Electronics and Telecommunications, Kraków, Poland.
[p] LIFAELS, La Salle, Universitat Ramon Llull, Barcelona, Spain.
[q] Hanoi University of Science, Hanoi, Viet Nam.
[r] Università di Padova, Padova, Italy.
[s] Università di Pisa, Pisa, Italy.
[t] Scuola Normale Superiore, Pisa, Italy.
[u] Università degli Studi di Milano, Milano, Italy.
[v] Politecnico di Milano, Milano, Italy.
[w] Associated to: Universidade Federal do Rio de Janeiro (UFRJ), Rio de Janeiro, Brazil.
[x] Associated to: Center for High Energy Physics, Tsinghua University, Beijing, China.
[y] Associated to: LPNHE, Université Pierre et Marie Curie, Université Paris Diderot, CNRS/IN2P3, Paris, France.
[z] Associated to: Physikalisches Institut, Ruprecht-Karls-Universität Heidelberg, Heidelberg, Germany.
[aa] Associated to: Institute of Theoretical and Experimental Physics (ITEP), Moscow, Russia.
[ab] Associated to: Universitat de Barcelona, Barcelona, Spain.
[ac] Associated to: Nikhef National Institute for Subatomic Physics, Amsterdam, The Netherlands.
[ad] Associated to: European Organization for Nuclear Research (CERN), Geneva, Switzerland.